

Single-spin azimuthal asymmetry in exclusive electroproduction of π^+ mesons

A. Airapetian,³¹ N. Akopov,³¹ Z. Akopov,³¹ M. Amarian,^{26,31} E.C. Aschenauer,⁷ H. Avakian,¹¹ R. Avakian,³¹ A. Avetissian,³¹ E. Avetissian,³¹ P. Bailey,¹⁵ V. Baturin,²⁴ C. Baumgarten,²¹ M. Beckmann,¹² S. Belostotski,²⁴ S. Bernreuther,²⁹ N. Bianchi,¹¹ H. Böttcher,⁷ A. Borissov,¹⁹ O. Bouhali,²³ M. Bouwuis,¹⁵ J. Brack,⁵ S. Brauksiepe,¹² A. Brüll,¹⁸ I. Brunn,⁹ H.J. Bulten,^{23,30} G.P. Capitani,¹¹ P. Chumney,²² E. Cisbani,²⁶ G. Ciullo,¹⁰ G.R. Court,¹⁶ P.F. Dalpiaz,¹⁰ R. De Leo,³ L. De Nardo,¹ E. De Sanctis,¹¹ D. De Schepper,² E. Devitsin,²⁰ P.K.A. de Witt Huberts,²³ P. Di Nezza,¹¹ M. Düren,¹⁴ M. Ehrenfried,⁷ G. Elbakian,³¹ F. Ellinghaus,⁷ J. Ely,⁵ R. Fabbri,¹⁰ A. Fantoni,¹¹ A. Fechtchenko,⁸ L. Felawka,²⁸ B.W. Filippone,⁴ H. Fischer,¹² B. Fox,⁵ J. Franz,¹² S. Frullani,²⁶ Y. Gärber,⁷ F. Garibaldi,²⁶ E. Garutti,²³ G. Gavrilo,²⁴ V. Gharibyan,³¹ G. Graw,²¹ O. Grebeniounk,²⁴ P.W. Green,^{1,28} L.G. Greeniaus,^{1,28} A. Gute,⁹ W. Haeberli,¹⁷ K. Hafidi,² M. Hartig,²⁸ D. Hasch,^{9,11} D. Heesbeen,²³ F.H. Heinsius,¹² M. Henocho,⁹ R. Hertenberger,²¹ W.H.A. Hesselink,^{23,30} G. Hofman,⁵ Y. Holler,⁶ R.J. Holt,¹⁵ B. Homme,¹³ G. Iarygin,⁸ A. Izotov,²⁴ H.E. Jackson,² A. Jgoun,²⁴ P. Jung,⁷ R. Kaiser,⁷ A. Kisselev,²⁴ P. Kitching,¹ K. Königsman,¹² H. Kolster,¹⁸ V. Korotkov,⁷ E. Kotik,¹ V. Kozlov,²⁰ B. Krauss,⁹ V.G. Krivokhijine,⁸ G. Kyle,²² L. Lagamba,³ A. Laziev,^{23,30} P. Lenisa,¹⁰ P. Liebing,⁷ T. Lindemann,⁶ W. Lorenzon,¹⁹ A. Maas,⁷ N.C.R. Makins,¹⁵ H. Marukyan,³¹ F. Masoli,¹⁰ K. McIlhany,^{4,18} F. Meissner,²¹ F. Menden,¹² V. Mexner,²³ N. Meyners,⁶ O. Mikloukho,²⁴ R. Milner,¹⁸ V. Muccifora,¹¹ A. Nagaitsev,⁸ E. Nappi,³ Y. Naryshkin,²⁴ A. Nass,⁹ K. Negodaeva,⁷ W.-D. Nowak,⁷ K. Oganessyan,^{6,11} T.G. O'Neill,² B.R. Owen,¹⁵ S.F. Pate,²² S. Podiathev,⁹ S. Potashov,²⁰ D.H. Potterveld,² M. Raithel,⁹ G. Rakness,⁵ V. Rappoport,²⁴ R. Redwine,¹⁸ D. Reggiani,¹⁰ P. Reimer,² A.R. Reolon,¹¹ K. Rith,⁹ D. Robinson,¹⁵ A. Rostomyan,³¹ D. Ryckbosch,¹³ Y. Sakemi,²⁹ I. Sanjiev,^{2,24} F. Sato,²⁹ I. Savin,⁸ C. Scarlett,¹⁹ A. Schäfer,²⁵ C. Schill,¹² F. Schmidt,⁹ G. Schnell,²² K.P. Schüller,⁶ A. Schwind,⁷ J. Seibert,¹² B. Seitz,¹ T.-A. Shibata,²⁹ V. Shutov,⁸ M.C. Simani,^{23,30} A. Simon,¹² K. Sinram,⁶ E. Steffens,⁹ J.J.M. Steijger,²³ J. Stewart,^{2,16,28} U. Stösslein,⁵ K. Suetsugu,²⁹ S. Taroian,³¹ A. Terkulov,²⁰ S. Tessarin,¹⁰ E. Thomas,¹¹ B. Tipton,⁴ M. Tytgat,¹³ G.M. Urciuoli,²⁶ J.F.J. van den Brand,^{23,30} G. van der Steenhoven,²³ R. van de Vyver,¹³ M.C. Vetterli,^{27,28} V. Vikhrov,²⁴ M.G. Vinciter,¹ J. Visser,²³ J. Volmer,⁷ C. Weiskopf,⁹ J. Wendland,^{27,28} J. Wilbert,⁹ T. Wise,¹⁷ S. Yen,²⁸ S. Yoneyama,²⁹ and H. Zohrabian³¹

(The HERMES Collaboration)

¹Department of Physics, University of Alberta, Edmonton, Alberta T6G 2J1, Canada

²Physics Division, Argonne National Laboratory, Argonne, Illinois 60439-4843, USA

³Istituto Nazionale di Fisica Nucleare, Sezione di Bari, 70124 Bari, Italy

⁴W.K. Kellogg Radiation Laboratory, California Institute of Technology, Pasadena, California 91125, USA

⁵Nuclear Physics Laboratory, University of Colorado, Boulder, Colorado 80309-0446, USA

⁶DESY, Deutsches Elektronen-Synchrotron, 22603 Hamburg, Germany

⁷DESY Zeuthen, 15738 Zeuthen, Germany

⁸Joint Institute for Nuclear Research, 141980 Dubna, Russia

⁹Physikalisches Institut, Universität Erlangen-Nürnberg, 91058 Erlangen, Germany

¹⁰Istituto Nazionale di Fisica Nucleare, Sezione di Ferrara and

Dipartimento di Fisica, Università di Ferrara, 44100 Ferrara, Italy

¹¹Istituto Nazionale di Fisica Nucleare, Laboratori Nazionali di Frascati, 00044 Frascati, Italy

¹²Fakultät für Physik, Universität Freiburg, 79104 Freiburg, Germany

¹³Department of Subatomic and Radiation Physics, University of Gent, 9000 Gent, Belgium

¹⁴Physikalisches Institut, Universität Gießen, 35392 Gießen, Germany

¹⁵Department of Physics, University of Illinois, Urbana, Illinois 61801, USA

¹⁶Physics Department, University of Liverpool, Liverpool L69 7ZE, United Kingdom

¹⁷Department of Physics, University of Wisconsin-Madison, Madison, Wisconsin 53706, USA

¹⁸Laboratory for Nuclear Science, Massachusetts Institute of Technology, Cambridge, Massachusetts 02139, USA

¹⁹Randall Laboratory of Physics, University of Michigan, Ann Arbor, Michigan 48109-1120, USA

²⁰Lebedev Physical Institute, 117924 Moscow, Russia

²¹Sektion Physik, Universität München, 85748 Garching, Germany

²²Department of Physics, New Mexico State University, Las Cruces, New Mexico 88003, USA

²³Nationaal Instituut voor Kernfysica en Hoge-Energiefysica (NIKHEF), 1009 DB Amsterdam, The Netherlands

²⁴Petersburg Nuclear Physics Institute, St. Petersburg, Gatchina, 188350 Russia

²⁵Institut für Theoretische Physik, Universität Regensburg, 93040 Regensburg, Germany

²⁶Istituto Nazionale di Fisica Nucleare, Sezione Roma 1, Gruppo Sanità
and Physics Laboratory, Istituto Superiore di Sanità, 00161 Roma, Italy

²⁷Department of Physics, Simon Fraser University, Burnaby, British Columbia V5A 1S6, Canada

²⁸TRIUMF, Vancouver, British Columbia V6T 2A3, Canada

²⁹Department of Physics, Tokyo Institute of Technology, Tokyo 152, Japan

³⁰*Department of Physics and Astronomy, Vrije Universiteit, 1081 HV Amsterdam, The Netherlands*

³¹*Yerevan Physics Institute, 375036, Yerevan, Armenia*

(Dated: April 16, 2002)

A single-spin asymmetry in the distribution of exclusively produced π^+ mesons azimuthally around the virtual photon direction relative to the lepton scattering plane has been measured for the first time in deep-inelastic scattering of positrons off longitudinally polarized protons. Integrated over the experimental acceptance, the $\sin\phi$ moment of the polarization asymmetry of the cross section is measured to be -0.18 ± 0.05 (stat.) ± 0.02 (syst.). The asymmetry is also studied as a function of the relevant kinematic variables, and its magnitude is found to grow with decreasing x and increasing $-t$ and vanish at $t \rightarrow t_{min}$ (where x is the Bjorken scaling variable and t is the squared four-momentum transferred to the nucleon).

PACS numbers: 13.60.-r, 13.60.Le, 13.85.Fb, 13.88.+e

The interest in hard exclusive processes has grown since a QCD factorization theorem was proved for the hard exclusive production of mesons by longitudinal virtual photons (helicity 0) [1]. The Generalized Parton Distribution functions (GPDs) [2, 3] appearing in this factorization scheme are of great interest because they can be related to parton angular momentum distribution functions that are not directly constrained or inaccessible through semi-inclusive or inclusive measurements [4, 5].

While unpolarized GPDs (typically designated as E and H) can be probed through exclusive vector meson production, polarized GPDs (typically designated as \tilde{E} and \tilde{H}) can be probed through exclusive pseudoscalar meson production without the need for a polarized target or beam. However, only a quadratic combination of GPDs appears in the unpolarized cross section for exclusive meson electroproduction, and so several independent observables are needed to disentangle the various distributions [6]. Additional observables can be accessed through the measurement of the polarized cross section. For example, it has been predicted [7] that for the exclusive production of π^+ mesons from a transversely polarized target by longitudinal virtual photons, the interference between the pseudoscalar (\tilde{E}) and pseudovector (\tilde{H}) amplitudes leads to a large target-related single-spin asymmetry in the distribution of the angle ϕ . Here ϕ is the azimuthal angle of the pion around the virtual photon momentum relative to the lepton scattering plane. The predicted asymmetry is of order unity. Moreover, the scaling region of this asymmetry (where corrections proportional to powers of $1/Q$ are small) is reached at lower Q^2 of the virtual photon than for the absolute cross section [8]. It has also been shown that corrections that are next-to-leading order (NLO) in α_s cancel in the transverse asymmetry [9]. No factorization theorem has been proved for transverse virtual photons (helicity ± 1), but their contribution to the cross section is predicted to be suppressed by at least a power of $1/Q$ [1].

In the case of electroproduction from a target polarized *longitudinally* with respect to the lepton beam momentum, a small transverse component (S_\perp) of the target polarization orthogonal to the virtual photon direction does appear, along with the dominant longitudinal com-

ponent (S_\parallel). The polarized cross section (σ_S) for this reaction has the form [10, 11]

$$\sigma_S \sim [S_\perp \sigma_\mathcal{L} + S_\parallel \sigma_\mathcal{L}\mathcal{T}] A_{\text{UL}}^{\sin\phi} \sin\phi, \quad (1)$$

where $A_{\text{UL}}^{\sin\phi}$ is the $\sin\phi$ moment of the polarization asymmetry. The subscripts U and L indicate the use of an unpolarized beam and longitudinally polarized target, respectively. Equation (1) shows that in the case of a longitudinally polarized target an additional term appears which contains the interference of longitudinal (\mathcal{L}) and transverse (\mathcal{T}) virtual photon amplitudes. Since a factorization theorem was not proved yet for transverse virtual photons quantitative predictions for this term would require a calculation in next-to-leading twist [9].

This letter reports on the first measurement of a single-spin asymmetry in the exclusive reaction $e^+ + \vec{p} \rightarrow e'^+ + n + \pi^+$. The relevant kinematic variables of this process in the target rest frame are the space-like squared four-momentum $-Q^2$ of the exchanged virtual photon with energy ν , the squared four-momentum t transferred to the nucleon, the Bjorken scaling variable $x \equiv Q^2/2M\nu$, where M is the proton mass, and the azimuthal angle ϕ described above. The sign of ϕ is given by $(e^{\vec{\tau}} \times e^{\vec{\tau}'}) \cdot \vec{\pi}^{\vec{\tau}} / |(e^{\vec{\tau}} \times e^{\vec{\tau}'}) \cdot \vec{\pi}^{\vec{\tau}}|$.

The data were collected in 1997 using a longitudinally polarized hydrogen gas target in the 27.6 GeV HERA positron storage ring at DESY. While the lepton beam was usually polarized oppositely to its direction, a small data sample taken with parallel beam polarization has shown that the measured asymmetry is independent of the lepton beam polarization. The average target polarization was 0.88 with a fractional uncertainty of 5% [12]. The scattered positron and the produced hadron were detected by the HERMES spectrometer [13]. Positrons were distinguished from hadrons with an average efficiency of 99% and a hadron contamination of less than 1% using the information from an electromagnetic calorimeter, a transition radiation detector, a preshower scintillator detector, and a threshold Čerenkov detector. The kinematic requirements imposed on the scattered positrons were $Q^2 > 1 \text{ GeV}^2$, $0.02 < x < 0.8$ and an invariant mass squared of the initial photon-nucleon system $W^2 > 4 \text{ GeV}^2$.

The recoiling neutron was not detected, and so exclusive production of mesons was selected by requiring that the missing mass (M_X) of the reaction $e^+ + p \rightarrow e'^+ + \pi^+ + X$ corresponded to the nucleon mass. The missing mass distribution for π^+ is shown in Fig. 1a (filled circles), for the pion momentum range from 4.9 to 14.0 GeV. These cuts on the pion's momentum serve only to restrict to a kinematic region in which the Čerenkov detector provides pion identification, and were not used in any other part of the analysis. A large number of events is observed in the missing mass region around the nucleon mass. However, from the π^+ missing mass distribution alone, it is not possible to separate the exclusive channel $e^+ + p \rightarrow e'^+ + \pi^+ + n$ from the neighboring (defined as non-exclusive) channels $\pi^+ + \Delta^0$, $\pi^+ + (N\pi)$ and $\pi^+ + (N\pi\pi)$, which can be smeared into the $\pi^+ + n$ region due to the limited experimental resolution. The histogram which is represented by a solid line in Fig. 1a is an arbitrarily normalized Monte Carlo simulation of the detector response to exclusive π^+ generated according to the predictions of refs. [14, 15] for the HERMES kinematics. It yields an experimental M_X resolution for the exclusive π^+ channel of about 230 MeV, which is larger than the separation from the non-exclusive channels mentioned before. The latter ones are also present in the $e^+ + p \rightarrow e'^+ + \pi^- + X$ process and are shown in Fig. 1a as empty circles, while exclusive π^- production with a nucleon in the final state is forbidden by charge conservation. As for π^+ , also non-exclusive π^- events are smeared into the exclusive region. Therefore, the non-exclusive π^+ background was estimated from the normalized number of π^- passing the same cuts as the π^+ and found in the same exclusive missing mass region.

In Fig. 1b, the difference between the π^+ and π^- missing mass distributions is shown, after normalizing the integral of the π^- distribution with respect to the π^+ one in the range $1.3 < M_X < 2.0$ GeV. This interval sees strong contributions from non-exclusive background from both resonant ($\pi^+ + \Delta^0$) and non-resonant ($\pi^+ + (N\pi)$ and $\pi^+ + (N\pi\pi)$) channels. The resulting background normalization factor is about 1.6, with a systematic uncertainty of 13%. The systematic uncertainty was estimated by using different normalization regions i.e. $1.2 < M_X < 1.5$ GeV and $2.0 < M_X < 2.5$ GeV. The difference between the π^+ and π^- missing mass distributions shows a clear peak centered at the nucleon mass. The curve in Fig. 1b is a Gaussian fit to the data. The deficit seen in the distribution at $M_X \approx 1.2 - 1.6$ GeV is due to a difference in the relative contribution of the resonant and non-resonant channels to the π^+ and π^- yields.

The ϕ dependence of the polarized cross section appears in the cross section asymmetry for exclusively produced π^+ , which is defined by

$$A(\phi) = \frac{1}{|S|} \frac{N_e^\uparrow(\phi) - N_e^\downarrow(\phi)}{N_e^\uparrow(\phi) + N_e^\downarrow(\phi)}. \quad (2)$$

Here N_e represents the yield of exclusive π^+ , the superscript \uparrow (\downarrow) denotes a target polarization direction

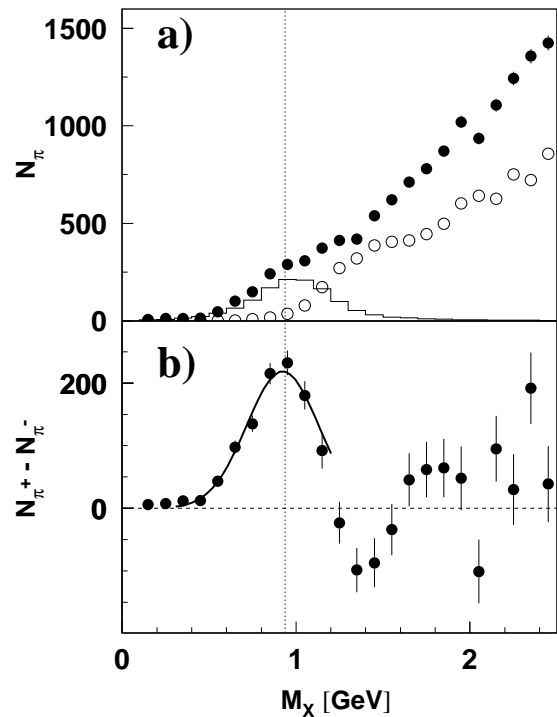


FIG. 1: a) Missing mass distribution for π^+ (filled circles) and π^- (empty circles) electroproduction at HERMES. The histogram is a Monte Carlo prediction for exclusive π^+ production with arbitrary normalization. b) Difference between the π^+ and normalized π^- distributions (see text). The curve is a Gaussian fit to the data for $0.4 < M_X < 1.2$ GeV. The vertical dotted line indicates the nucleon mass. The error bars represent the statistical uncertainties.

anti-parallel (parallel) to the positron beam momentum, and S is the degree of polarization of the target protons. All the tracks identified as hadrons were assumed to be pions, as the requirement that the missing mass corresponds to the nucleon mass removes all the hadrons heavier than the pion from the data sample. An analysis requiring pion identification by the Čerenkov detector was performed and gave similar results but with reduced statistics.

To evaluate the asymmetry defined by equation (2), a background correction has been applied. The total number of events $N(\phi)$ in each bin is the sum of exclusive events $N_e(\phi)$ and background events $N_{bg}(\phi)$. Equation (2) can thus be written

$$A(\phi) = \frac{1}{|S|} \frac{N^\uparrow(\phi) - N^\downarrow(\phi) - |S|A_{bg}(\phi)N_{bg}(\phi)}{N^\uparrow(\phi) + N^\downarrow(\phi) - N_{bg}(\phi)} \quad (3)$$

where $A_{bg}(\phi) = \frac{1}{|S|} \frac{N_{bg}^\uparrow(\phi) - N_{bg}^\downarrow(\phi)}{N_{bg}^\uparrow(\phi) + N_{bg}^\downarrow(\phi)}$ is the asymmetry of the background. As shown in equation (3), only two parameters are needed to correct for background processes: the background yield, $N_{bg}(\phi) = N_{bg}^\uparrow(\phi) + N_{bg}^\downarrow(\phi)$, and its asymmetry, $A_{bg}(\phi)$. As discussed earlier, the background

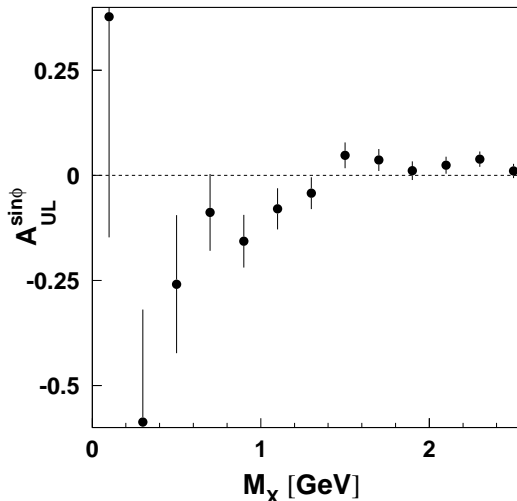


FIG. 2: $A_{UL}^{\sin\phi}$ for the $e^+ + \vec{p} \rightarrow e'^+ + h^+ + X$ reaction as a function of missing mass. The error bars represent the statistical uncertainties.

yield in each bin was estimated from the normalized number of π^- events passing all the cuts applied to π^+ events. Since the background originates from the smearing of events occurring at higher missing mass, the background asymmetry was estimated to be the asymmetry from the neighboring missing mass region where the contribution of exclusive π^+ events is negligible. The $\sin\phi$ moment of the uncorrected asymmetry ($A(\phi)$ in equation (3) with $N_{bg} = 0$) is shown in Fig. 2 as a function of M_X . All the other moments were found to be compatible with zero. In the missing mass region from 1.3 to 2.0 GeV, $A_{UL}^{\sin\phi}$ ranges between -0.05 and $+0.05$ with an average value of 0.019 ± 0.014 . This asymmetry is compatible with that measured for semi-inclusive π^+ production [16]. Therefore the $\sin\phi$ moment of the background asymmetry has been taken conservatively to be 0 ± 0.1 . It is important to stress that the exclusive asymmetry computed by means of equation (3) (i.e. after background correction) is independent of the missing mass cut within the range $0.7 < M_X < 1.5$ GeV, despite the fact that the signal-to-background ratio (N_e/N_{bg}) goes from 20 to 0.8 in the same interval. However, a missing mass cut has been applied to optimize the statistical accuracy. For a cut at high missing mass the statistical error on $A(\phi)$ given by equation (3) is dominated by the statistics of the background sample. For a cut at low missing mass it is determined by the (reduced) number of exclusive events. The best statistical accuracy is obtained by requiring $M_X < 1.05$ GeV. For this cut, the inferred signal to background ratio is about 6 and therefore, the result depends only weakly on any systematic uncertainty of the background yield or its asymmetry. All the results presented in this paper were obtained by requiring $M_X < 1.05$ GeV.

The cross section asymmetry integrated over x , Q^2 and

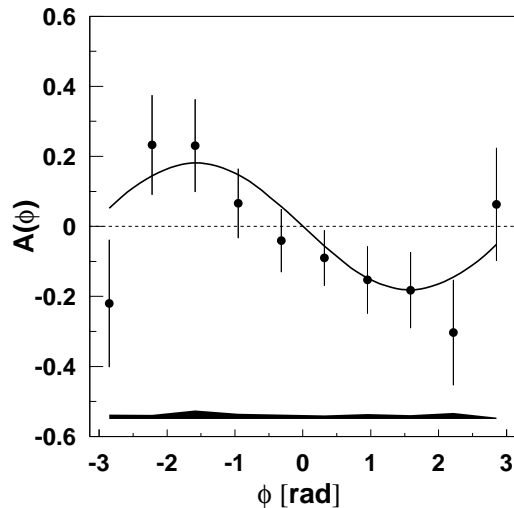


FIG. 3: Cross section asymmetry $A(\phi)$ averaged over x , Q^2 , and t for the reaction $e^+ + \vec{p} \rightarrow e'^+ + n + \pi^+$. The curve is the best fit to the data by $A(\phi) = A_{UL}^{\sin\phi} \cdot \sin\phi$ with $A_{UL}^{\sin\phi} = -0.18 \pm 0.05$ at a reduced χ^2 of 0.8. The error bars and bands represent the statistical and systematic uncertainties, respectively.

t is shown in Fig. 3. The average values of the kinematic variables are $\langle x \rangle = 0.15$, $\langle Q^2 \rangle = 2.2$ GeV² and $\langle t \rangle = -0.46$ GeV² (with 75% of the events occurring at $|t| < 0.5$ GeV²). The data show a large asymmetry in the distribution versus azimuthal angle ϕ , with a clear $\sin\phi$ dependence. A fit to this dependence of the form

$$A(\phi) = A_{UL}^{\sin\phi} \cdot \sin\phi \quad (4)$$

yields $A_{UL}^{\sin\phi} = -0.18 \pm 0.05 \pm 0.02$ with a reduced χ^2 of 0.8. The background correction described above and its associated uncertainty account for -0.024 ± 0.011 (syst) in this value. A fit to $A(\phi)$ using a more general function $A(\phi) = a \sin\phi + b \sin 2\phi + c \cos\phi + d \cos 2\phi$ yields values for b , c , and d that are compatible with zero, showing the dominant role of the $\sin\phi$ contribution. The results of this fit are listed in Table I. The band in Fig. 3 represents the systematic uncertainty from background yield and asymmetry, and from target polarization. It has been shown by a Monte Carlo simulation [17] of exclusive events that the momentum resolution of the HERMES spectrometer does not affect the magnitude of the measured asymmetry over the kinematic range of the measurement, and that acceptance effects cancel in equation (2).

Current theoretical calculations [7–9] for a transversely polarized target are in agreement with each other and predict a large asymmetry. The transverse component of the target polarization in the virtual photon frame is

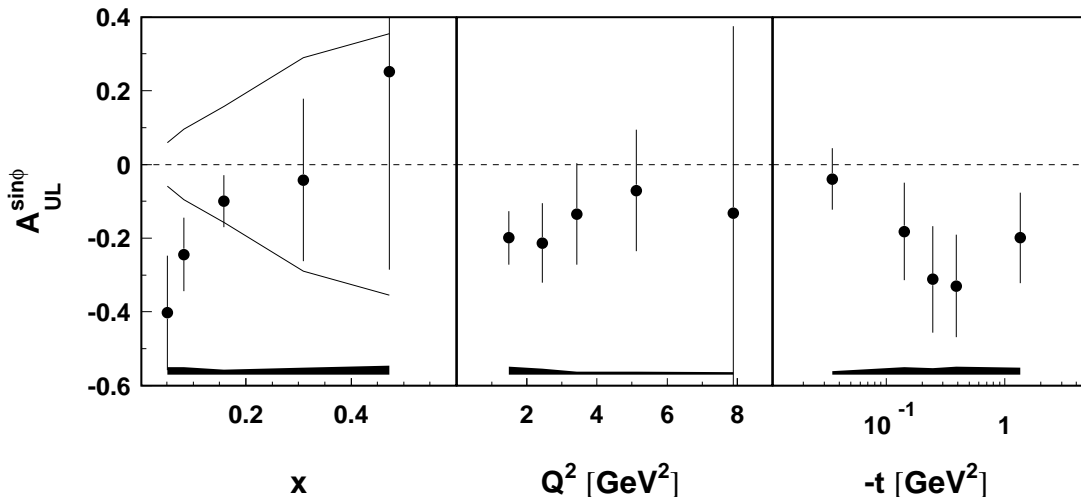


FIG. 4: Kinematic dependence of $A_{UL}^{\sin\phi}$ on the variables x , Q^2 , and t for the reaction $e^+ + \vec{p} \rightarrow e'^+ + n + \pi^+$. The error bars and bands represent the statistical and systematic uncertainties, respectively. The solid lines show the upper limits for any asymmetry arising from the transverse target polarization component.

given by

$$S_{\perp} = |S| \sin\theta_{\gamma} = |S| \sqrt{\frac{4M^2 x^2}{Q^2 + 4M^2 x^2} \left(1 - y - \frac{M^2 x^2 y^2}{Q^2}\right)}, \quad (5)$$

where θ_{γ} is the virtual photon emission angle, E is the lepton beam energy and $y = \nu/E$ is the fraction of the lepton's energy carried off by the virtual photon. The average value of $\sin\theta_{\gamma}$ for the present measurement is 0.16. As discussed before, estimates for the asymmetry arising from the longitudinal component of the target polarization are not yet available.

The dependence of $A_{UL}^{\sin\phi}$ on the individual kinematic variables x , Q^2 , and t is shown in Fig. 4 and reported in Table II. The table shows that these three kinematic quantities are strongly correlated by the experimental conditions. The absolute magnitude of the asymmetry shows a clear rise with decreasing x . The values of the relative transverse target polarization component ($\langle \sin\theta_{\gamma} \rangle$) are given in Table II and shown with both signs by the two full lines in the first panel of Fig. 4, indicating the limits for any asymmetry arising from that component. At low x the asymmetry must arise from the longitudinal target polarization component, independent of any model. No strong Q^2 dependence is observed within the statistical accuracy. Finally, the asymmetry is seen to increase in absolute magnitude with $-t$ and vanish in the forward limit ($t \rightarrow t_{min}$), where the pion momentum becomes collinear to the virtual photon momentum.

In summary, a single-spin azimuthal asymmetry has been measured for the first time in the exclusive electroproduction of π^+ mesons from a longitudinally polarized proton target. The measured asymmetry is large and negative. The dependence of this asymmetry on the kinematic

a	b	c	d
-0.19 ± 0.06	0.05 ± 0.05	-0.03 ± 0.05	-0.03 ± 0.05

TABLE I: Results of the fit of $A(\phi)$ (Fig. 3) to the form $A(\phi) = a \sin\phi + b \sin 2\phi + c \cos\phi + d \cos 2\phi$. The reduced χ^2 is 0.9.

variables x , Q^2 , and t has been investigated, and its magnitude is found to increase at low x and at large $|t|$. Further, the data show that the longitudinal target polarization component with respect to the virtual photon direction provides the dominant contribution to the measured asymmetry at small x . A next-to-leading twist calculation would thus be required for a complete description of the measurement. The present data, in combination with future HERMES measurements on a transversely polarized target [18] for which a large asymmetry is expected, opens the way to experimentally disentangle the asymmetry arising from the two target polarization components. This information may provide a first glimpse of certain unknown Generalized Parton Distributions.

We thank M. Diehl, M. Guidal, D. Müller, G. Piller, M.V. Polyakov, M. Strikman, and O. Teryaev for many interesting discussions on this subject. We gratefully acknowledge the DESY management for its support and the DESY staff and the staffs of the collaborating institutions. This work was supported by the FWO-Flanders, Belgium; the Natural Sciences and Engineering Research Council of Canada; the INTAS and TMR network contributions from the European Community; the German Bundesministerium für Bildung und Forschung; the Deutsche Forschungsgemeinschaft (DFG); the Deutscher Akademischer Austauschdienst (DAAD);

	$\langle x \rangle$	$\langle Q^2 \rangle$ [GeV ²]	$\langle \sin \theta_\gamma \rangle$	$A_{UL}^{\sin \phi}$
x				
0.05		1.3	0.06	$-0.40 \pm 0.16 \pm 0.02$
0.08		1.6	0.10	$-0.24 \pm 0.10 \pm 0.02$
0.16		2.6	0.16	$-0.10 \pm 0.07 \pm 0.01$
0.31		3.6	0.29	$-0.04 \pm 0.22 \pm 0.02$
0.47		5.0	0.36	$0.25 \pm 0.54 \pm 0.02$
Q^2 [GeV ²]				
1.5	0.12		0.15	$-0.20 \pm 0.07 \pm 0.02$
2.4	0.17		0.17	$-0.21 \pm 0.11 \pm 0.02$
3.4	0.21		0.17	$-0.13 \pm 0.14 \pm 0.01$
5.1	0.26		0.16	$-0.07 \pm 0.17 \pm 0.01$
7.9	0.38		0.19	$-0.13 \pm 0.51 \pm 0.01$
$-t$ [GeV ²]				
0.04	0.11	2.2	0.11	$-0.04 \pm 0.08 \pm 0.01$
0.14	0.13	2.4	0.13	$-0.18 \pm 0.13 \pm 0.02$
0.25	0.14	2.3	0.14	$-0.31 \pm 0.15 \pm 0.02$
0.39	0.16	2.5	0.16	$-0.33 \pm 0.14 \pm 0.02$
1.34	0.24	2.8	0.24	$-0.20 \pm 0.12 \pm 0.02$

TABLE II: $A_{UL}^{\sin \phi}$ as a function of x , Q^2 , and t .

the Italian Istituto Nazionale di Fisica Nucleare (INFN); Monbuscho International Scientific Research Program, JSPS, and Toray Science Foundation of Japan; the Dutch Foundation for Fundamenteel Onderzoek der Materie (FOM); the U.K. Particle Physics and Astronomy Research Council; and the U.S. Department of Energy and National Science Foundation.

-
- [1] J.C. Collins *et al.*, Phys. Rev. D **56**, 2982 (1997).
[2] D. Müller, D. Robaschik, B. Geyer, F.-M. Dittes, and J. Horejsi, Fortschr. Phys. **42**, 101 (1994).
[3] A.V. Radyushkin Phys. Rev. D **56**, 5524 (1997).
[4] X. Ji, Phys. Rev. Lett. **78**, 610 (1997).
[5] K. Goeke, M.V. Polyakov, and M. Vanderhaeghen, Prog. Part. Nucl. Phys. **47**, 2001 (401) and references therein.
[6] M. Diehl, SLAC-PUB-8670, hep-ph/0010200.
[7] L.L. Frankfurt, M.V. Polyakov, M. Strikman, and M. Vanderhaeghen, Phys. Rev. Lett. **84**, 2589 (2000).
[8] L.L. Frankfurt, P.V. Pobylitsa, M.V. Polyakov, and M. Strikman, Phys. Rev. D **60**, 014010 (1999).
[9] A.V. Belitsky, and D. Müller, Phys. Lett. B **513**, 349 (2001).
[10] M.V. Polyakov, and M. Vanderhaeghen, Proceedings DIS 2000, Ed. J.A. Gracey and T. Greenshaw, World Scientific.
[11] M. Diehl, Talk given at the *Ringberg Workshop on New Trends in HERA Physics 2001*, June 17-22, 2001, Tegernsee, Germany, hep-ph/0109040.
[12] HERMES Collaboration, A. Airapetian *et al.*, Phys. Lett. B **442**, 484 (1998).
[13] HERMES Collaboration, K. Ackerstaff *et al.*, Nucl. Instrum. Methods A **417**, 230 (1998).
[14] L. Mankiewicz, G. Piller, and A. Radyushkin, Eur. Phys. J. C **10**, 307 (1999).
[15] M. Vanderhaeghen, P.A.M. Guichon, and M. Guidal, Phys. Rev. D **60**, 094017 (1999).
[16] HERMES Collaboration, A. Airapetian *et al.*, Phys. Rev. Lett. **84**, 4047 (2000).
[17] E. Thomas (on behalf of the HERMES Collaboration), Talk given at the *Workshop on Deep Inelastic Scattering (DIS 2001)*, Apr 27 - May 1, 2001, Bologna, Italy.
[18] W.-D. Nowak (on behalf of the HERMES Collaboration), Talk given at the *Workshop on Deep Inelastic Scattering (DIS 2001)*, Apr 27 - May 1, 2001, Bologna, Italy, hep-ex/0108021.